Journal of Biomedical Optics

SPIEDigitalLibrary.org/jbo

Differences in fluorescence profiles from breast cancer tissues due to changes in relative tryptophan content via energy transfer: tryptophan content correlates with histologic grade and tumor size but not with lymph node metastases

Laura A. Sordillo
Peter P. Sordillo
Yury Budansky
Yang Pu
Robert R. Alfano

Differences in fluorescence profiles from breast cancer tissues due to changes in relative tryptophan content via energy transfer: tryptophan content correlates with histologic grade and tumor size but not with lymph node metastases

Laura A. Sordillo, Peter P. Sordillo, Yury Budansky, Yang Pu, and Robert R. Alfano*
The City College of the City University of New York, Institute for Ultrafast Spectroscopy and Lasers, Department of Physics, 160 Convent Avenue, New York, New York 10031, United States

Abstract. The correlation between histologic grade, an increasingly important measure of prognosis for patients with breast cancer, and tryptophan levels from tissues of 15 breast carcinoma patients was investigated. Changes in the relative content of key native organic biomolecule tryptophan were seen from the fluorescence spectra of cancerous and paired normal tissues with excitation wavelengths of 280 and 300 nm. Due to a large spectral overlap and matching excitation–emission spectra, fluorescence resonance energy transfer from tryptophan-donor to reduced nicotinamide adenine dinucleotides-acceptor was noted. We used the ratios of fluorescence intensities at their spectral emission peaks, or spectral fingerprint peaks, at 340, 440, and 460 nm. Higher ratios correlated strongly with high histologic grade, while lower-grade tumors had low ratios. Large tumor size also correlated with high ratios, while the number of lymph node metastases, a major factor in staging, was not correlated with tryptophan levels. High histologic grade correlates strongly with increased content of tryptophan in breast cancer tissues and suggests that measurement of tryptophan content may be useful as a part of the evaluation of these patients. [DOI: 10.1117/1.JBO.19.12.125002]

Keywords: fluorescence spectroscopy; breast carcinoma; tryptophan; histologic grade; tumor size; reduced nicotinamide adenine dinucleotides; collagen; ultraviolet light; energy transfer; optical biopsy; lymph node metastases; hormone receptor status.

Paper 140611RR received Sep. 23, 2014; accepted for publication Nov. 24, 2014; published online Dec. 18, 2014.

1 Introduction

Tumor histologic grade is a recognized, but underappreciated, predictor of prognosis in breast cancer patients.[1–3] Despite the importance of grade, it has historically not been included as one of the criteria for staging of this cancer. The current TNM staging system for breast carcinoma utilizes only tumor size and extent of local invasion (T), number of axillary lymph nodes with metastases (N), and presence of distant metastases (M) as measures of the stage of the cancer.[4] As a result, patient prognosis (and thus the need for adjuvant chemotherapy) is often assessed using only these measures. Rakha et al.[1] noted, however, that tumor histologic grade is at least as important an indicator of patient prognosis as the number of lymph node metastases and is more important than tumor size. In a review of 22,616 patients with breast cancer, Henson et al.[5] found that patients with low-grade cancers and sizes less than 2 cm had a 99% 5-year survival despite the presence of lymph node metastases. In another study of patients with estrogen-receptor positive breast cancer and one to three positive axillary lymph nodes, the 10-year relapse rate was 43% for high-grade tumors, but only 24% and 5% for intermediate- and low-grade cancers.[6]

In 1984, Alfano et al.[7,8] showed that optical spectroscopy could be used as an alternative technique to detect cancer by determining the different emission properties of key organic biomolecules in the tissue. Fluorescence spectroscopy using excitation wavelengths from the ultraviolet light region, for example, can highlight key biomolecules such as tryptophan, reduced nicotinamide adenine dinucleotides (NADH), and collagen in the tissue. It has been reported that cancerous tissue samples have an increased amount of the amino acid tryptophan (emission intensity peak maximum at ~340 nm) compared with collagen or NADH (emission intensity peaks maxima at ~380 and ~440 nm, respectively).[9–17] Most recently, Zhang et al.[17] showed, using fluorescence spectroscopy, that increased tryptophan is linked to an aggressive cancer cell line. Tryptophan is required for protein synthesis and thus increased fluorescent levels can be expected in cancerous breast tissue due to higher cell density and uncontrolled cell division. Recently, the spectral fingerprints of tissues from patients with different breast cancer histologies were examined using a novel fluorescence device known as the S^3-LED ratiometer unit and an LED excitation wavelength of 280 nm.[15,16] In those reports, we showed consistently higher ratios of the 340 over 440 nm and 340 over 460 nm emission intensity peaks in malignant samples of breast cancer patients compared with their paired normal samples, regardless of the characteristics of the patient's cancer.[15]

At an excitation of 280 nm, aromatic amino acids (phenylalanine, tyrosine, and tryptophan residues) can be excited; however, the emission is most likely from the indole ring of tryptophan. Tyrosine and phenylalanine will contribute significantly

*Address all correspondence to: Robert R. Alfano, E-mail: alfano@sci.ccny.cuny.edu

0091-3286/2014/$25.00 © 2014 SPIE

less to the overall emission at this excitation due to fluorescent quenching attributed to the energy transfer of phenylalanine to tyrosine and tyrosine to tryptophan. Apart from an intraprotein energy transfer from phenylalanine to tyrosine, phenylalanine is unlikely to produce fluorescence energy transfer due to a low-quantum yield. Similarly, tyrosine can be quenched due to an energy transfer from tyrosine to tryptophan residues. Therefore, tryptophan residues dominate emission and are ideal for fluorescence resonance energy transfer. At a selective longer-wavelength excitation of 300 nm, only tryptophan residues in proteins will be excited.[18] From these excitation wavelengths, the longer-wavelength (red-shifted) ^1L_a emitting state of tryptophan will occur at a maximum emission intensity peak of ~340 nm. Additional contributions to the emission spectra at these excitations can occur from proximal fluorophores in the tissue such as NADH (a highly fluorescent coenzyme with absorption and emission peaks at 340 and 440 to 460 nm, respectively). Table 2 highlights the absorption and emission peaks of key organic biomolecules in tissue. Due to a large spectral overlap and matching excitation–emission spectra, fluorescent resonance energy transfer from excited tryptophan (donor) to NADH (acceptor) (a dipole–dipole interaction shown by Förster to be an interaction of coupled electronic dipoles known as donor and acceptor molecules) can occur and affect the overall fluorescent spectrum of tryptophan. Studies by Torikata et al.[19,20] have shown that energy transfer from tryptophan to neighboring NADH in pig lactate dehydrogenase and malate dehydrogenase causes a decrease in its fluorescence lifetimes and leads to quenching of tryptophan fluorescence.

In this study, the spectral emission profiles from 15 patients with breast carcinoma were obtained using the conventional LS 50 Perkin-Elmer luminescence spectrometer with excitations at 280 and 300 nm. Dual excitation wavelengths were used to show energy transfers among key fluorophores. These spectral profiles were analyzed using a combination of emission intensity peak ratios. We used the ratios of fluorescence intensities at their spectral emission peaks, or spectral fingerprint peaks, at 340, 440, and 460 nm. The relative intensities or ratios (R) of emission intensity peaks, from these excitations, at 340, 440, and 460 nm from malignant (M) tissue samples ($R_{M1} = I_{340}/I_{440}$ and $R_{M2} = I_{340}/I_{460}$) and from paired normal (N) tissue samples ($R_{N1} = I_{340}/I_{440}$ and $R_{N2} = I_{340}/I_{460}$) were calculated. The extent of the increase in tryptophan was measured from the ratios of cancerous ratios (R_{M1} and R_{M2}) over normal ratios (R_{N1} and R_{N2}) to give $R_1 = R_{M1}/R_{N1}$ and $R_2 = R_{M2}/R_{N2}$. We report that increased tryptophan levels demonstrated by increases in R_1 and R_2 correlate strongly with high histologic grade and with large tumor size, but not with lymph node metastases, or with estrogen receptor, progesterone receptor, or HER-2-Neu receptor statuses. This suggests that measurement of tryptophan content may be useful as a part of the evaluation of patients with breast cancer.

2 Experiment

2.1 *Tissue Specimen*

Spectral profiles were acquired from 30 breast tissue samples from 15 breast cancer patients (15 cancerous and 15 paired

Table 1 Characteristics of 15 breast cancer patients.

Patient number (n)	Age (years)	Grade	Tumor size (cm)	Number of nodes	Histology
1	63	3	4.8	1	Invasive ductal carcinoma
2	66	3	2.5	4	Invasive ductal carcinoma
3	59	3	2.8	4	Invasive ductal carcinoma
4	54	1	2.2	>10	Invasive ductal carcinoma
5	59	3	5.4	>10	Invasive ductal carcinoma
6	74	3	8.5	16	Micropapillary breast carcinoma
7	61	3	4.0	11	Multifocal invasive ductal carcinoma
8	76	3	4.5	Not sampled	Invasive ductal carcinoma
9	48	2	3.5	2	Invasive lobular carcinoma, pleomorphic variant
10	51	3	*	*	Recurrent invasive ductal carcinoma
11	62	2	1.8	>10	Invasive ductal carcinoma, lobular features
12	53	3	3.0	1	Invasive ductal carcinoma
13	60	1	0.9	1	Invasive ductal carcinoma
14	57	3	2.7	0	Invasive ductal carcinoma
15	64	2	4.1	1	Invasive carcinoma with ductal and lobular features

* Not assessed, recurrent cancer.

Table 2 Absorption and emission peak maxima of key organic biomolecules.

Molecules	Tyrosine	Tryptophan	Collagen	Elastin	NADH	Flavins
Absorption peak maximum (nm)	275	280 to 300	325	325	340	450
Emission peak maximum (nm)	280 to 300	340	400	410	440 to 460	525

normal samples). Tissue samples were supplied by the National Disease Research Interchange and the Cooperative Human Tissue Network under an Institutional Review Board protocol. None of the samples were chemically treated (no phosphate buffer saline immersion). The samples were kept on ice except during the experiments. The tissues from paired normal and malignant samples were done under the same exact conditions. In general, the tissue samples were analyzed within 24 h of resection. The malignant sample and its paired normal sample were always done at the same time. The patient ages ranged from 48 to 76 years old (Table 1). Three were premenopausal, 11 were post-menopausal, and 1 was peri-menopausal. Fourteen were Caucasian and one was Black. One had received prior neo-adjuvant chemotherapy without shrinkage of the tumor, while 14 were treatment naïve. One patient ($n = 10$) had had a prior surgery and the sample analyzed was a recurrent cancer. Characteristics of the 15 cancers patient are given in Table 1. Measurements were acquired from multiple random locations along the surfaces of the samples. Cuvettes were used to hold tissue samples.

2.2 *Optical Setups*

2.2.1 *LS 50 fluorescence spectrometer*

The conventional LS 50 Perkin Elmer luminescence spectrometer is a computer controlled device which uses a Xenon (Xe) discharge lamp light source. It is equipped with excitation, emission, and synchronous scan functions in the spectral range of 200 to 800 nm and has ±1-nm wavelength accuracy. The slit widths can be varied to give resolutions between 2 and 15 nm. The emission spectra from the tissue samples were acquired using excitation wavelengths of 280 and 300 nm, with a 280- and 300-nm full-width half-maximum 25 ± 5 nm bandpass filters. The focal spot size of the excitation beam is approximately 7 mm in length and 2 mm in width.

3 Results and Discussion

Spectral profiles from patients with breast carcinoma were acquired using the LS 50 fluorescence spectrometer at 280 and 300 nm excitations. Table 2 highlights the optimal absorption

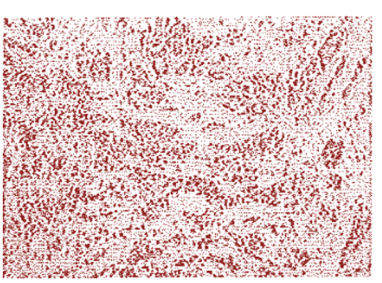

(a)

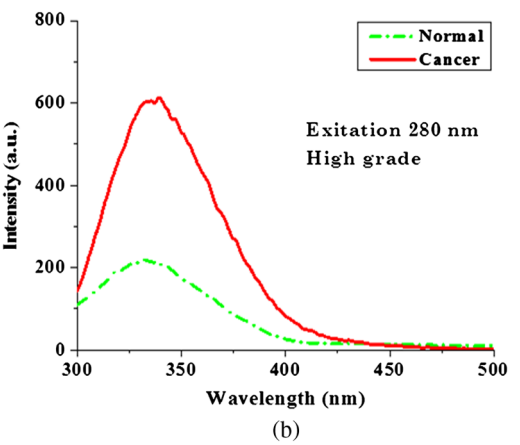

(b)

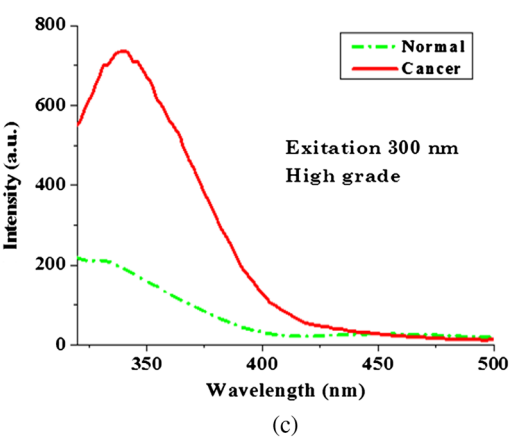

(c)

Fig. 1 (a) Microscopic image of the pathology slide (20× magnified) from malignant breast tissue from patient $n = 10$; and (b) and (c) corresponding fluorescent spectra from malignant (MAL) and normal (NORM) breast tissues after 280 and 300 nm excitations.

and emission peak maxima of key organic biomolecules tyrosine, tryptophan, collagen, elastin, NADH, and flavins. With light at excitation peak wavelength maxima of 280 to 300 nm, biomolecules in tissue such as tryptophan, collagen, and NADH will absorb this Gaussian-shaped excitation spectrum of light and emit a spectrum of light due to a combination of biomolecules with peak maxima at ~340, 380, and 440 to 460 nm (largely due to tryptophan, collagen, and NADH, respectively). The most intense of these peaks (due to tryptophan) is located at ~340 nm. A weak secondary peak at 440 to 460 nm is due to NADH and is said to occur due to resonance energy transfer of protein–NADH complexes.[18–22] A large spectral overlap and matching excitation–emission peaks at 340 nm from tryptophan and NADH, respectively, make tryptophan and NADH a good donor–acceptor pair. The Förster distance $\bar{R}_0$ for this pair in solution has been reported as 25 Å [where $\bar{R}_0$ is obtained using the average value of the orientation factor (angle between the donor and acceptor dipoles) κ^2, where $\kappa^2 = \bar{\kappa}^2 = 2/3$ to account for the fast-rotatory Brownian motion which occurs during the lifetime of the donor].[23]

Figure 1(a) is a microscopic image of the pathology slide (20× magnified) from malignant breast tissue from patient $n = 10$. The breast cancer sample from this patient with invasive ductal carcinoma was grade 3 (high grade) and this correlates with higher ratios of emission peaks. Figures 1(b) and 1(c) show the corresponding average fluorescence spectra from normal and malignant breast tissue samples with excitations of 280 and 300 nm. A peak emission maximum can be seen at ~340 nm in both the malignant and normal samples. This result is consistent with previous studies.[15,16] The emission spectra show similar peak maxima at ~340 nm using an excitation of 280 and 300 nm and suggest that the fluorescence is dominated by tryptophan residues.

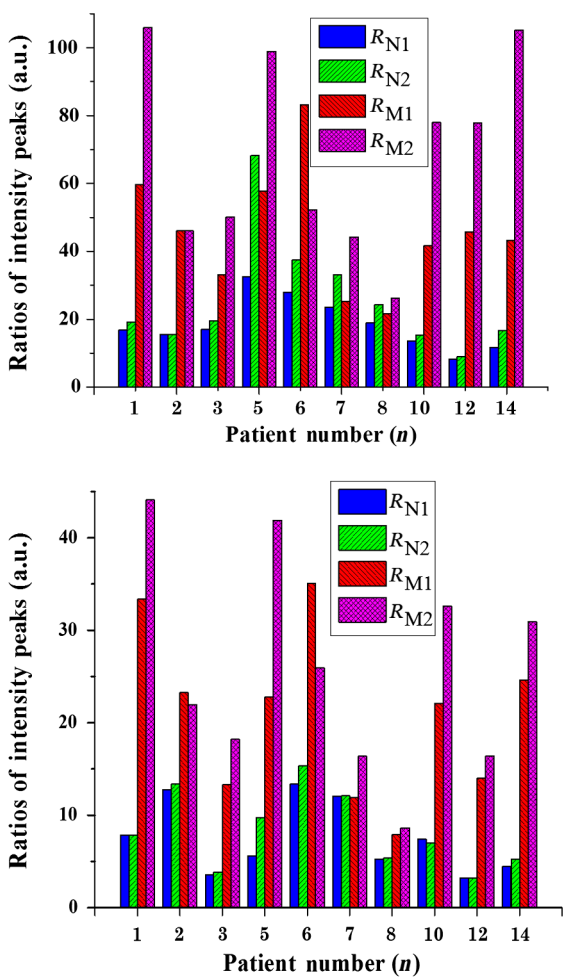

Fig. 2 (a) and (b) Normalized ratios R_{M1}, R_{M2}, R_{N1}, and R_{N2} from high-grade tumors with intensity peaks at excitations 280 and 300 nm, respectively, using the LS 50 spectrometer.

Ratios (R) of emission intensity peak maxima from biomolecules in malignant ($R_{M1} = I_{340}/I_{440}$and $R_{M2} = I_{340}/I_{460}$) and normal ($R_{N1} = I_{340}/I_{440}$ and $R_{N2} = I_{340}/I_{460}$) samples were calculated. Figures 2(a) and 2(b) show that R_{M1} and R_{M2} from patients with high-grade breast cancer have higher bar graphs than R_{N1} and R_{N2} from excitations 280 and 300 nm. These figures demonstrate that malignant tissue samples have higher 340 over 440 nm and 340 over 460 nm ratios compared with corresponding ratios from their paired normal tissue samples.

Normalized, averaged, and cancerous over normal ratios ($R_1 = R_{M1}/R_{N1}$ and $R_2 = R_{M2}/R_{N2}$) are given in Tables 3 and 4, respectively. Tables 3 and 4 compare the histologic grade with ratio results R_1 and R_2. Patients with high histologic grade breast cancer had higher R_1, whereas patients with intermediate-/low-grade breast cancer had lower R_1 results. R_1 for high-grade tumors, from 280 and 300 nm excitations, had average values of 2.77608 (with standard deviation of 1.36389 and p-value of $0.00138 < 0.05$) and 2.910345 (with standard deviation of 1.49592 and p-value of $0.00260 < 0.05$).

Similar results can be seen for R_2, with a higher overall R_2 for patients with high-grade cancer and a lower R_2 for patients with intermediate-/low-grade cancer. R_2 for high-grade tumors,

Table 3 Normalized ratios (R_1) of emission intensity peaks from $R_{M1} = I_{340}/I_{440}$ over $R_{N1} = I_{340}/I_{440}$.

Patient number (n)	Grade	Excitation 280 nm	Excitation 300 nm
1	High	3.55559	4.24868
2	High	2.97966	1.81906
3	High	1.94209	3.68094
5	High	1.77844	1.45143
6	High	2.97260	2.62358
7	High	1.06760	0.98885
8	High	1.14453	1.50294
10	High	3.04503	2.97847
12	High	5.58090	4.30446
14	High	3.69436	5.50504
4	Low or intermediate	0.96124	1.03272
9	Low or intermediate	0.51636	1.10069
11	Low or intermediate	0.93561	1.00690
13	Low or intermediate	1.03057	0.69261
15	Low or intermediate	0.78371	0.86216

Table 4 Normalized ratios (R_2) of emission intensity peaks from $R_{M2} = I_{340}/I_{460}$ over $R_{N2} = I_{340}/I_{460}$.

Patient number (n)	Grade	Excitation 280 nm	Excitation 300 nm
1	High	5.52591	5.63311
2	High	2.97966	1.64052
3	High	2.57668	4.71759
5	High	4.06914	4.29812
6	High	1.39372	1.68522
7	High	1.33370	1.35229
8	High	1.07624	1.61274
10	High	5.11103	4.64725
12	High	8.65770	5.08158
14	High	6.29456	5.90878
4	Low or intermediate	0.88474	1.06531
9	Low or intermediate	0.55638	0.44834
11	Low or intermediate	1.18821	1.15523
13	Low or intermediate	1.20407	0.52290
15	Low or intermediate	0.88429	0.85510

from 280 and 300 nm excitations, had average values of 3.90183 (with standard deviation of 2.49327 and p-value of $0.00484 < 0.05$) and 3.65772 (with a standard deviation of 1.759722 and p-value of $0.00081 < 0.05$). The averages of ratios R_1 and R_2 were 3.31149 for high-grade tumors and 0.88436 for low-grade tumors. Higher ratios correlated strongly with grade 3 (high) histologic grade, while tumors that were grade 2 or 1 (intermediate/low) demonstrated low ratios.

Large tumor size also correlated with high ratios. This is not surprising as tumor size frequently correlates with the degree of tumor grade.[1] Exceptions to the association of high ratios and large tumor sizes occurred where the tumor was lower grade ($n = 9$ and 15) and the histologic grade could be regarded as a confounder. Tables 5 and 6 compare the tumor size with the ratios R_1 and R_2.

With the exception of $n = 9$ and 15, the average of R_1 and R_2, from 280 and 300 nm excitations at different tumor sizes, was 2.99007 with a standard deviation of 1.16402 (above 4.5 cm), 3.41884 with a standard deviation of 2.32900 (2.5 to 4.5 cm), and 0.98116 with a standard deviation of 0.20324 (0 to <2.5 cm).

Although histologic grade and tumor size (to a lesser degree) correlate with high ratios, the number of axillary lymph node metastases, a major determinant of staging, was found not to correlate with the ratios, with tumors from patients who had a small number or zero positive nodes demonstrating high ratios if high grade, and tumors from patients with a large number of positive nodes showing low ratios if they were lower grade. For example, analysis of the samples from patient $n = 14$ showed high R_1 and R_2 because the cancer was high grade, despite the

Table 5 Correlation between tumor size and ratio ($R_1 = R_{M1}/R_{N1}$) of emission intensity peaks from $R_{M1} = I_{340}/I_{440}$ over $R_{N1} = I_{340}/I_{440}$.

Patient number (n)	Tumor size (cm)	Excitation 280 nm	Excitation 300 nm
1	Above 4.5	3.55559	4.24868
5	Above 4.5	1.77844	1.45143
6	Above 4.5	2.97260	2.62358
2	2.5 to 4.5	2.97966	1.81906
3	2.5 to 4.5	1.94209	3.68094
7	2.5 to 4.5	1.06760	0.99885
8	2.5 to 4.5	1.14453	1.50294
9[a]	2.5 to 4.5	0.51636	0.37816
12	2.5 to 4.5	5.58090	4.30446
14	2.5 to 4.5	3.69436	5.50504
15[a]	2.5 to 4.5	0.78371	0.86216
4	0 to <2.5	0.96124	1.03272
11	0 to <2.5	0.93561	1.10069
13	0 to <2.5	1.03057	0.69261

[a]Low-grade tumor, grade acts as a confounder.

Table 6 Correlation between tumor size and ratio ($R_2 = R_{M2}/R_{N2}$) of emission intensity peaks from $R_{M2} = I_{340}/I_{460}$ over $R_{N2} = I_{340}/I_{460}$.

Patient number (n)	Tumor size (cm)	Excitation 280 nm	Excitation 300 nm
1	Above 4.5	3.55559	4.24868
5	Above 4.5	4.06914	4.29812
6	Above 4.5	1.39372	1.68522
2	2.5 to 4.5	2.97966	1.64052
3	2.5 to 4.5	2.57668	4.71759
7	2.5 to 4.5	1.33370	1.35229
8	2.5 to 4.5	1.07624	1.61274
9[a]	2.5 to 4.5	0.55638	0.44834
12	2.5 to 4.5	8.65770	8.08158
14	2.5 to 4.5	6.29456	5.90878
15[a]	2.5 to 4.5	0.88429	0.85510
4	0 to <2.5	0.88474	1.06531
11	0 to <2.5	1.18821	1.15523
13	0 to <2.5	1.20407	0.52290

[a]Low-grade tumor, grade acts as a confounder.

fact that this patient had zero positive lymph nodes. The sample from patient $n = 12$ demonstrated a high ratio presumably because it was high grade, despite the fact that only one lymph node was positive for cancer. On the other hand, analysis of samples $n = 4, 7$, and 11 gave low ratios presumably because their cancers were lower grade, despite the fact that each of these patients had more than 10 positive lymph nodes. No correlation of increased ratios could be found with estrogen receptor, progesterone receptor, or HER-2-Neu receptor statuses.

4 Conclusion

A number of researchers have shown that cancerous tissues have an increase in their tryptophan content compared with normal tissues and cells.[9–17] The emission spectra show similar peak maxima at ~340 nm using an excitation of 280 and 300 nm and suggest that the fluorescence is dominated by tryptophan residues. We note possible energy transfer between tryptophan (donor) and NADH (acceptor) in breast tissue samples with excitation wavelengths of 280 and 300 nm. Further studies are needed in order to determine the tryptophan residues involved in this event and the efficiency of such an energy transfer. We also report that the increase in tryptophan content is correlated with the degree of tumor histologic grade. Indeed, the difference in tryptophan content between higher and lower grade tumors that we observed in our study was marked. The averages of ratios R_1 and R_2 were 3.31149 for high-grade tumors and 0.88436 for low-grade tumors. Tumor size also correlates with increased tryptophan content, but this appears to be due to the known association of large tumor size with high histologic grade.[1] As histologic grade is becoming recognized as an increasingly important measure of prognosis for patients with breast carcinoma, the measurement of tryptophan ratios may also be useful in the assessment of these cancers. Further studies will be needed to determine whether very high breast cancer tryptophan levels in those patients with high-grade tumors might carry a worse prognosis, and thus necessitate more aggressive treatment than would be done in patients with only slightly elevated levels.

References

1. E. A. Rakha et al., "Breast cancer prognostic classification in the molecular era: the role of histological grade," *Breast Cancer Res.* **12**(4), 207 (2010).
2. G. J. R. Porter et al., "Patterns of metastatic breast carcinoma: influence of tumor histological grade," *Clin. Radiol.* **59**(12), 1094–1098 (2004).
3. I. Soerjomataram et al., "An overview of prognostic factors for long-term survivors of breast cancer," *Breast Cancer Res. Treat.* **107**, 309–330 (2008).
4. S. B. Edge et al., *AJCC Cancer Staging Manual*, 7th ed., pp. 347–376, Springer, New York (2010).
5. D. E. Henson et al., "Relationship among outcome, stage of disease, and histologic grade for 22,616 cases of breast cancer. The basis for a prognostic index," *Cancer* **68**(10), 2142–2149 (1991).
6. E. A. Rakka et al., "Prognostic significance of Nottingham histologic grade in invasive breast carcinoma," *J. Clin. Oncol.* **26**, 3153–3158 (2008).
7. R. R. Alfano et al., "Laser induced fluorescence spectroscopy from native cancerous and normal tissue," *IEEE J. Quantum Electron.* **20**, 1507–1511 (1984).
8. R. R. Alfano et al., "Light sheds light on cancer," *Bull. N. Y. Acad. Med.* **67**, 143–150 (1991).
9. A. Tankiewicz et al., "Tryptophan and its metabolites in patients with oral squamous cell carcinoma: preliminary study," *Adv. Med. Sci.* **51**(Suppl 1), 221–224 (2006).
10. F. V. DeGeorge and R. R. Brown, "Differences in tryptophan metabolism between breast cancer patients with and without cancer at other sites," *Cancer* **26**, 767–770 (1970).
11. B. Banerjee et al., "Tryptophan autoflorescence imaging of neoplasms of the human colon," *J. Biomed. Opt.* **17**(1), 016003 (2012).
12. Y. Yang et al., "Optical spectroscopy of benign and malignant breast tissues," *Lasers Life Sci.* **7**, 115–127 (1996).
13. P. K. Gupta, S. K. Majumder, and A. Uppal, "Breast cancer diagnosis using N2 laser excited autoflorescence spectroscopy," *Laser Surg. Med.* **21**(5), 417–422 (1997).
14. Y. Pu et al., "Changes of collagen and nicotinamide adenine dinucleotide in human cancerous and normal prostate tissues studied using native fluorescence spectroscopy with selective excitation wavelength," *J. Biomed. Opt.* **15**(4), 047008 (2010).
15. L. A. Sordillo et al., "Optical spectral fingerprints of tissues from patients with different breast cancer histologies using a novel fluorescence spectroscopic device," *Technol. Cancer Res. Treat.* **12**, 455–461 (2013).
16. L. A. Sordillo et al., "Compact Stokes shift and fluorescence spectroscopic diagnostics LED ratiometer unit with no moving parts for cancer detection," *Proc. SPIE* **8220**, 82200I (2012).
17. L. Zhang et al., "Tryptophan as the fingerprint for distinguishing aggressiveness among breast cancer cell lines using native fluorescence spectroscopy," *J. Biomed. Opt.* **19**(3), 037005 (2014).
18. J. R. Lakowicz, *Principles of Fluorescence Spectroscopy*, Kluwer Academics/Plenum Publisher, New York (1999).
19. T. Torikata et al., "Lifetimes and NADH quenching of tryptophan fluorescence in pig heart lactate dehydrogenase," *Biochemistry* **18**(2), 385–390 (1979).
20. T. Torikata et al., "Lifetimes and NADH quenching of tryptophan fluorescence in pig heart cytoplasmic malate dehydrogenase," *J. Biol. Chem.* **254**(9), 3516–3520 (1979).
21. C. C. Fields, W. T. Birdsong, and R. H. Goodman, "Differential binding of NAD^+ and NADH allows the transcriptional corepressor carboxyl-terminal binding protein to serve as a metabolic sensor," *Proc. Natl. Acad. Sci. U. S. A.* **100**(16), 9202–9207 (2003).
22. M. J. Kronman and L. G. Holmes, "The fluorescence of native, denatured and reduced-denatured proteins," *Photochem. Photobiol.* **14**(2), 113–134 (1971).
23. I. Z. Steinberg, "Long-range nonradiative transfer of electronic excitation energy in proteins and polypeptides," *Annu. Rev. Biochem.* **40**, 83–11 (1971).

Laura A. Sordillo is a researcher at the Institute for Ultrafast Spectroscopy and Lasers in the Department of Physics at The City College of CUNY. She has developed a novel portal device for the assessment of cancerous lesions, studied the use of an octreotate indocyanine dye to target breast cancer, and investigated the use of the three NIR optical windows to image microfractures of human tibial bone. She is a recipient of the CCNY-MSKCC Partnership Graduate Award.

Peter P. Sordillo is a physician and cancer researcher, whose specialty is the treatment of extremely rare cancers. He also holds graduate degrees in philosophy and in physics. He is currently an attending hematologist and oncologist at Lenox Hill Hospital and research consultant at the Institute for Ultrafast Spectroscopy and Lasers in the Department of Physics at The City College of CUNY.

Yang Pu obtained his PhD degree in electrical engineering at the City University of New York. He is a multidisciplinary researcher in the fields of biomedical optics. His research is concentrated on breaking two limits of optics: 1) enhancing the resolution of microscope to break the limitation of diffraction, and 2) imaging deep organs from large animal and human using optical techniques.

Robert R. Alfano is a distinguished professor of Science and Engineering at The City College of CUNY. He has pioneered many applications of light and photonics technologies to the study of biological, biomedical, and condensed matter systems and invented and used in his research supercontinuum and novel tunable solid state lasers. He received his PhD degree in physics from New York University and is a Fellow of the American Physical Society, Optical Society of America, and IEEE.

Yury Budansky: Biography is not available.